▮▮▮▮▮▮▮▮▮▮▮▮

Results on Charm Hadroproduction from CERN Experiment WA82

The WA82 Collaboration

M. Adamovich[5], Y. Alexandrov[5], R. Anselmi[3], F. Antinori[2], D. Barberis[2], W. Beusch[2],
A. Buys[4], V. Casanova[3], M. Dameri[3], M. Davenport[2], J.P. Dufey[2], A. Forino[1],
B.R. French[2], R. Gessaroli[1], F. Grard[4], K. Harrison[2], R. Hurst[3], A. Jacholkowski[2],
S. Kharlamov[5], A. Kirk[2], E. Lamanna[2], J.C. Lassalle[2], P. Legros[4], P. Mazzanti[1],
F. Muller[2†], P. Nechaeva[5], P. Novelli[3], B. Osculati[3], A. Quareni[1], N. Redaelli[2],
C. Roda[2], L. Rossi[3], G. Tomasini[3], F. Viaggi[1†], M. Weymann[2] and M. Zavertyaev[5]

1   Dipartimento di Fisica and INFN, Bologna, Italy.
2   CERN, European Organization for Nuclear Research, Geneva, Switzerland.
3   Dipartimento di Fisica and INFN, Genova, Italy.
4   Université de Mons-Hainaut and IISN, Mons, Belgium.
5   Lebedev Physical Institute, Moscow, Russia.
†   Deceased.

Presented by: F. Antinori, CERN,

at ICHEP 92, Dallas, Texas, USA, August 1992

Abstract

Experiment WA82 has collected data from 1987 to 1989 with the Ω' spectrometer at the CERN SPS. The aim of WA82 was a high statistics study of charm hadroproduction, using a silicon microstrip vertex detector and an impact parameter trigger. Latest results on the nuclear dependence of charm production and on the x_F distributions of D^+ and D^- mesons are presented and discussed.

1. Introduction

One of the main open problems in charm physics is the relative importance of perturbative and non-perturbative QCD phenomena in the hadronic production of charm mesons. The nuclear dependence of charm hadroproduction and the longitudinal distributions of charm hadrons are two main benchmarks in this respect: perturbative QCD predicts a linear rise of the charm hadroproduction cross section with the mass number of the target nucleus, and if perturbative QCD alone were at play one would expect the x_F distributions for all charm hadrons to reproduce those of the c and $\bar{c}$ quarks, and therefore to be all very similar.

Experiment WA82 was run at the CERN Ω' spectrometer. The experiment was based on a silicon microstrip telescope, which allowed triggering and off-line detection of secondary vertices. The collected charm sample, consisting of about 3000 fully reconstructed decays, has allowed study of the production and decay mechanisms of charm hadrons.

In section 2 some features of the experimental apparatus of WA82 relevant to the paper are briefly reviewed, the analysis chain and the data sample are treated in section 3. Section 4 is devoted to the description of the measurement of the nuclear dependence of charm hadroproduction, while the results on the x_F distributions of $D^{\pm}$ mesons are discussed in section 5. Section 6 contains the summary and the conclusions.

2. Experimental apparatus

The WA82 set-up is sketched in figure 1. π^- (340 GeV/c) or p (370 GeV/c) beams collided on a 2 mm target, which was divided vertically into two portions of different materials (W/Si or W/Cu depending on the runs) to allow the study of the nuclear dependence of charm production.

The silicon vertex detector [1] was 50 cm long and consisted of fourteen planes with pitches ranging from 10 μm to 50 μm. Eight additional 20 μm planes were used as beam detector. The typical accuracy on the measurement of the position of secondary vertices was 500 μm (longitudinal) and 30 μm (transverse).

The microstrip detectors were sitting inside the Ω' spectrometer, equipped with its standard multi-wire and drift chambers. The magnetic field intensity was 1.8 $Tesla$

at the center of the Ω magnet. The accuracy on the measurement of momenta was $(dp/p)_{MEAS} \simeq 3 \cdot 10^{-4} p(GeV)$, while the multiple scattering contribution was $(dp/p)_{SCAT} \simeq 10^{-3}$. The apparatus also featured a RICH detector and an electromagnetic calorimeter, which have not been used for the analysis presented in this paper.

Three vertex detector planes and one beam plane were also employed in the impact parameter trigger [2]: selecting events with at least one track with an impact parameter to the primary vertex in a range between 100 μm and 1000 μm, this trigger produced an enrichment factor of the charm sample of about 15.

3. Data analysis

WA82 took data in 1987, 1988 and 1989. The π^- beam was used in all three years, on a W/Si target in 1987 and 1988 ($1.8 \cdot 10^7$ triggers), and on W/Cu in 1989 ($3 \cdot 10^7$ triggers). In addition, a proton beam run was performed in 1988 (10^7 triggers).

The full data sample has been used for the analysis presented in this paper. The analysis chain started with a filter program, selecting events with evidence for secondary vertices using only the microstrip information in the non-bending projection. The events thus selected were passed through the full track and vertex space reconstruction program. Some cuts were applied in order to clean up the samples: the primary vertex of the event had to be reconstructed inside the target region; the secondary vertex had to be well separated from the primary vertex (at least 6 σ_{VTX} where $\sigma_{VTX} = \sigma_{PRIM} \oplus \sigma_{SEC}$) and from the target (at least 2 σ_{SEC}), and had to point back to the primary vertex within 60 μm. Vertices with an error on the calculated invariant mass bigger than 30 MeV/c^2 were rejected. The acceptance for D mesons of the apparatus, trigger and analysis chain extends to high x_F (as an example the $D^+ \rightarrow K^-\pi^+\pi^+$ x_F acceptance is shown in figure 2).

Figure 3 and figure 4 show invariant mass distributions for the main charm hadron decay channels from the pion- and proton-beam samples. Invariant mass peaks were fitted to gaussian shapes, and charm candidates were selected by invariant mass cuts of ± 3 fitted standard deviations (typically $\sigma_M = 5 \div 8$ MeV/c^2) around the fitted central value. The amount of background under the peaks was estimated by straight line fits. The results of two such fits are shown in figure 5. The final charm sample

thus obtained consists of some 3000 fully reconstructed charm hadrons.

4. Nuclear dependence of charm hadroproduction

The cross section for particle production on nuclei is usually parametrized as $\sigma(A) = \sigma_0 A^\alpha$. From a theoretical point of view, α should approach the surface value of $2/3$ for long distance phenomena (full screening), and the volume value of 1 for pointlike interactions (in particular $\alpha = 1$ is the prediction for perturbative QCD phenomena). Experimentally, $\alpha \simeq 3/4$ for the total hadron-nucleus cross section, and for strangeness production [3]. $\alpha \simeq 3/4$ has also been measured for charm production by some early beam dump experiments [4,5].

In WA82 the beam illuminates simultaneously the two halves (W and Si or Cu) of the target (see figure 6), this allows to eliminate several possible sources of systematic uncertainty in the measurement of $\alpha(D)$ [6].

In order to perform the calculation, the number of D mesons renconstructed in events with the primary vertex lying in each half of the target must be corrected for the relative luminosities on the two halves (measured by regular beam trigger sampling) and for the biases due to the trigger, the event reconstruction and the analysis (as determined by a detailed Monte Carlo).

As a control of our procedure we have performed the calculation of α for our K_S^0 sample. We obtained:

$$\alpha(K_S^0) = 0.72 \pm 0.02 \qquad for \qquad < x_F > = 0.05$$

in good agreement with published data [3,7].

The same procedure applied to the charm sample gives

$$\alpha(D) = 0.92 \pm 0.06 \qquad for \qquad < x_F > = 0.24$$

The error is dominated by statistics, and the systematic uncertainty arising from Monte Carlo corrections is small and is included in the quoted error. Recent open charm and J/ψ experiments [8] report α values ranging from 0.85 to 1.

There have been some indications that α may decrease with x_F in charm hadroproduction [8,9,10]. Our data, shown in figure 7, do not indicate, within the errors, any decrease of $\alpha(D)$ with x_F.

5. x_F distributions for D^+ and D^-

If the longitudinal distributions for charm mesons were to follow those of the produced charm quarks, i.e. if no non-perturbative phenomena were present, the x_F distributions for all D mesons should be similar, and in particular independent of the D meson light quark content.

Early results from NA27 [11,12] indicated enhancement of leading charmed mesons (charmed mesons containing a beam valence quark) at high x_F in π^- induced reactions. This "leading particle effect" has been confirmed by a beam dump experiment [13] but not by NA32 [14].

With a π^- ($\bar{u}d$) beam, D^+ ($c\bar{d}$) is non-leading, and D^- ($\bar{c}d$) is leading. The D^0 ($c\bar{u}$) and the $\bar{D}^0$ ($\bar{c}u$) cannot be unambiguously considered as respectively leading and non-leading: they are in the case of direct production, but if they are produced in resonance decay, their leading/non-leading character may be swapped (as for example in the decay $D^{*+}(c\bar{d}) \rightarrow D^0(c\bar{u}) + \pi^+(u\bar{d})$). This cannot happen in the $D^\pm$ case, as $D^{*0} \rightarrow D^+\pi^-$ decays are forbidden by energy conservation, and the remaining $D^{*+} \rightarrow D^+\pi^0$ and $D^{*+} \rightarrow D^+\gamma$ decays conserve the "leading-ness" of the charmed meson. For this reason only D^+ and D^- samples have been used in our analysis.

For the x_F distributions study, the D^+ and D^- candidates samples have been selected with $\pm 3\sigma_M$ cuts on the invariant mass distributions. Background samples have been defined as the contents of the two sidebands in the $K^-\pi^+\pi^+$ and $K^+\pi^-\pi^-$ invariant mass distributions going from 1740 MeV to 1830 MeV and from 1900 MeV to 2000 MeV, renormalized to the amount of background under the D^+ and D^- peaks. This background was then subtracted to the D^+ and D^- candidates x_F distributions. The resulting x_F distributions, uncorrected for acceptance, are plotted in figure 8. The $D^\pm$ sample thus selected consists of 358 ± 12 $D^+ \rightarrow K^-\pi^+\pi^+$, 515 ± 9 $D^- \rightarrow K^+\pi^-\pi^-$ from π^- interactions, and 97 ± 3 $D^\pm \rightarrow K^\mp\pi^\pm\pi^\pm$ from p interactions.

The $(D^- - D^+)/(D^- + D^+)$ distribution (figure 9) shows a clear excess of D^- over D^+, which increases with x_F. A statistical test on the D^- and D^+ distributions has been performed, combining a χ^2 test and a run test. The probability that the D^- and D^+ distributions be two random samplings of the same limit distribution is less than 5%. The acceptance corrected distributions for D^+ and D^- are shown in figure 10. After

acceptance correction, the integral excess of D^- over D^+ is

$$\frac{D^-}{D^+} = 1.38 \pm 0.13$$

The PYTHIA [15] event generator qualitatively reproduces this effect as a hadronization effect in the Lund string fragmentation model: at our energies the $\bar{d}$ quark necessary for building a D^+ meson must essentially be produced by string fragmentation. On the contrary a d quark in the forward hemisphere is very often present in the final state as a spectator quark from the beam π^-. Therefore there are additional ways for producing a D^- than a D^+, particularly at high x_F, near to the projectile rapidity, so an excess of D^- over D^+, increasing with increasing x_F is predicted by PYTHIA.

The $(D^- - D^+)/(D^- + D^+)$ distributions from WA82 and from PYTHIA are compared in figure 11. The exact amount of the effect is not reproduced by PYTHIA, which also predicts too large an integral value of the excess of D^- over D^+ (a factor 2, compared with our measured 1.38 ± 0.13).

The D^+ and D^- x_F distributions measured by WA82 are compared with the PYTHIA predictions in figures 12 and 13. Also shown are the $c/\bar{c}$ distributions from next-to-leading-order (NTLO) QCD calculations [16] (whose shape is compatible with that of the PYTHIA leading-order + parton shower $c/\bar{c}$ ones, not shown). The PYTHIA D^+ and the NTLO c quark x_F distributions are very similar, apart from a small deviation at high x_F. Both are compatible with our data within the experimental accuracy. A much more marked deviation of the PYTHIA charmed hadron distribution from the NTLO charmed quark distribution, due to the mechanism outlined above, is visible in the D^- case. WA82 D^- data lie in between the two.

In the proton beam case, the D^+ and D^- x_F distributions are compatible with each other within our statistics. The cumulative $D^\pm$ x_F distribution is plotted in figure 14 along with the PYTHIA prediction. The two curves are compatible, and steeper than the corresponding pion beam ones, as expected from the difference in the gluon structure functions, which are steeper in protons than in pions.

6

6. Summary and conclusions

We have studied the nuclear dependence of charm hadroproduction and the longitudinal distributions of D^+ and D^- mesons in $\sqrt{s} \simeq 25 \; GeV$ π^- - nucleus and p - nucleus interactions. We have measured a value of $\alpha(D) = 0.92 \pm 0.06$. There is no indication of a variation of $\alpha(D)$ with x_F in our data. A clear excess of D^- over D^+, increasing towards high x_F, is observed in the π^- beam sample. The measured integral excess is $D^-/D^+ = 1.38 \pm 0.13$, and the probability that the two x_F distributions be random samplings of the same limit distribution is less than 5%. Comparison with theory shows that the nuclear dependence of the integral charm production cross section is compatible within 1.5σ with the perturbative QCD prediction, while non-perturbative effects are probably required to explain the relative amounts and the longitudinal distributions of the different charmed mesons.

References

[1] M.Adamovich et al., Nucl. Inst. Meth. A309 (1991) 401.

[2] M.Adamovich et al., IEEE Trans. Nucl. Sci. 37 (1990) 236.

[3] D.S.Barton et al., Phys. Rev. D27 (1983) 2580.

[4] H.Cobbaert et al., Zeit. Phys. C36 (1987) 577.

[5] M.E.Duffy et al., Phys. Rev. Lett. 55 (1985) 1816.

[6] M.Adamovich et al., CERN/PPE 92-56, submitted to Phys. Lett. B.

[7] P.Skubic et al., Phys. Rev. D18 (1978) 3115.

[8] D.M.Alde et al., Phys. Rev. Lett. 66 (1991) 133.

[9] M.Mac Dermott and S.Reucroft, Phys. Lett. B184 (1987) 108.

[10] S.Kartik et al., Phys. Rev. D41 (1990) 41.

[11] M.Aguilar-Benitez et al., Phys. Lett. B168 (1986) 170.

[12] M.Aguilar-Benitez et al., Zeit. Phys. C31 (1986) 491.

[13] J.L.Ritchie et al., Phys. Lett. B138 (1984) 213.

[14] S.Barlag et al., CERN/EP 88-04.

[15] H.-U.Bengtsson and T.Sjöstrand, Comp. Phys. Comm. 46 (1987) 43.

[16] P.Nason, private communications.

Figure Captions

Fig. 1 Sketch of the WA82 set-up.

Fig. 2 WA82 x_F acceptance for $D^\pm \to K^\mp \pi^\pm \pi^\pm$.

Fig. 3 Some WA82 charm peaks. π^- data.

Fig. 4 Some WA82 charm peaks. p data.

Fig. 5 Invariant mass distributions fits for $D^+ \to K^- \pi^+ \pi^+$ and $D^- \to K^+ \pi^- \pi^-$.

Fig. 6 Transverse distribution of primary vertices in the target made of silicon and tungsten for the K^0_s and $D^- \to K^\mp \pi^\pm$ samples.

Fig. 7 $\alpha(D)$ measured in three x_F intervals.

Fig. 8 WA82 D^+ and D^- distributions for pion and proton data (uncorrected for acceptance).

Fig. 9 The WA82 $(D^- - D^+)/(D^- + D^+)$ asymmetry (π^- data).

Fig. 10 WA82 D^+ and D^- x_F distributions, acceptance corrected. (π^- data).

Fig. 11 Comparison of the WA82 and PYTHIA $(D^- - D^+)/(D^- + D^+)$ asymmetries. (π^- beam).

Fig. 12 D^+ x_F distributions in π^- - nucleon interactions from WA82 and PYTHIA. Also shown is the NTLO x_F distribution for c quarks.

Fig. 13 D^- x_F distributions in π^- - nucleon interactions from WA82 and PYTHIA. Also shown is the NTLO x_F distribution for $\bar{c}$ quarks.

Fig. 14 $D^\pm$ x_F distributions in p - nucleon interactions from WA82 and PYTHIA.

THE WA82 SETUP AT THE Ω' SPECTROMETER (CERN)

$\odot |B| = 1.8\ Tesla$

340 GeV/c π^-
370 GeV/c p

y
x

π/p
BEAM

BHY

TARGET

Ω' MWPC's

VERTEX DETECTOR

MY2
MY1

D.C. 1

D.C. 2

MY3
MY4
HZ1
HY1

-3   0   3   6   9   12   15m

3σ SEPARATION

π/K   UP TO   50 GeV/c
π/p   UP TO 100 GeV/c
K/p   UP TO 80 GeV/c

THRESHOLDS:

π : 4 GeV/c
p : 14 GeV/c
K : 26 GeV/c

RICH (1987 + 1988 ONLY)

HZ2

E.M.CALORIMETER
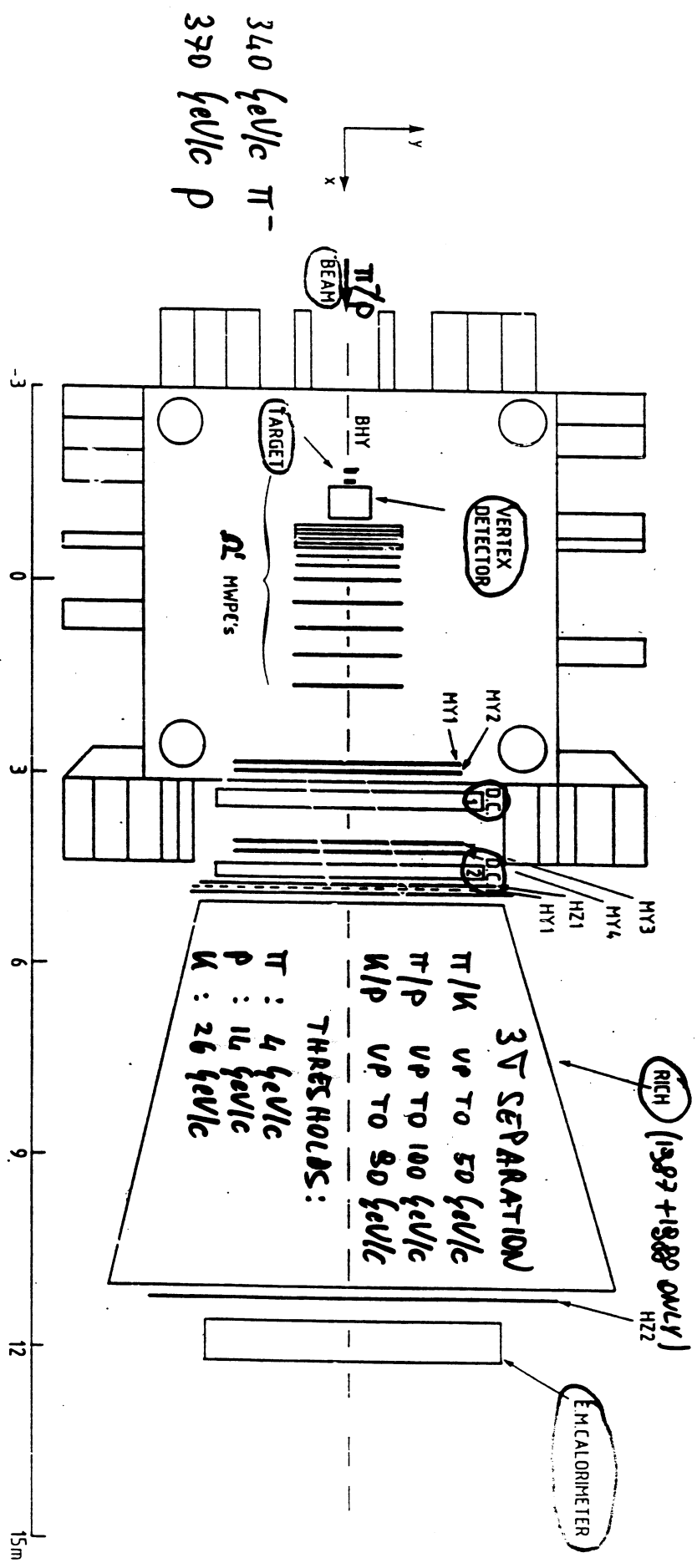
Fig. 1

WA82 x_F acceptance for $D^+ \rightarrow K^- \pi^+ \pi^+ + $ c.c.
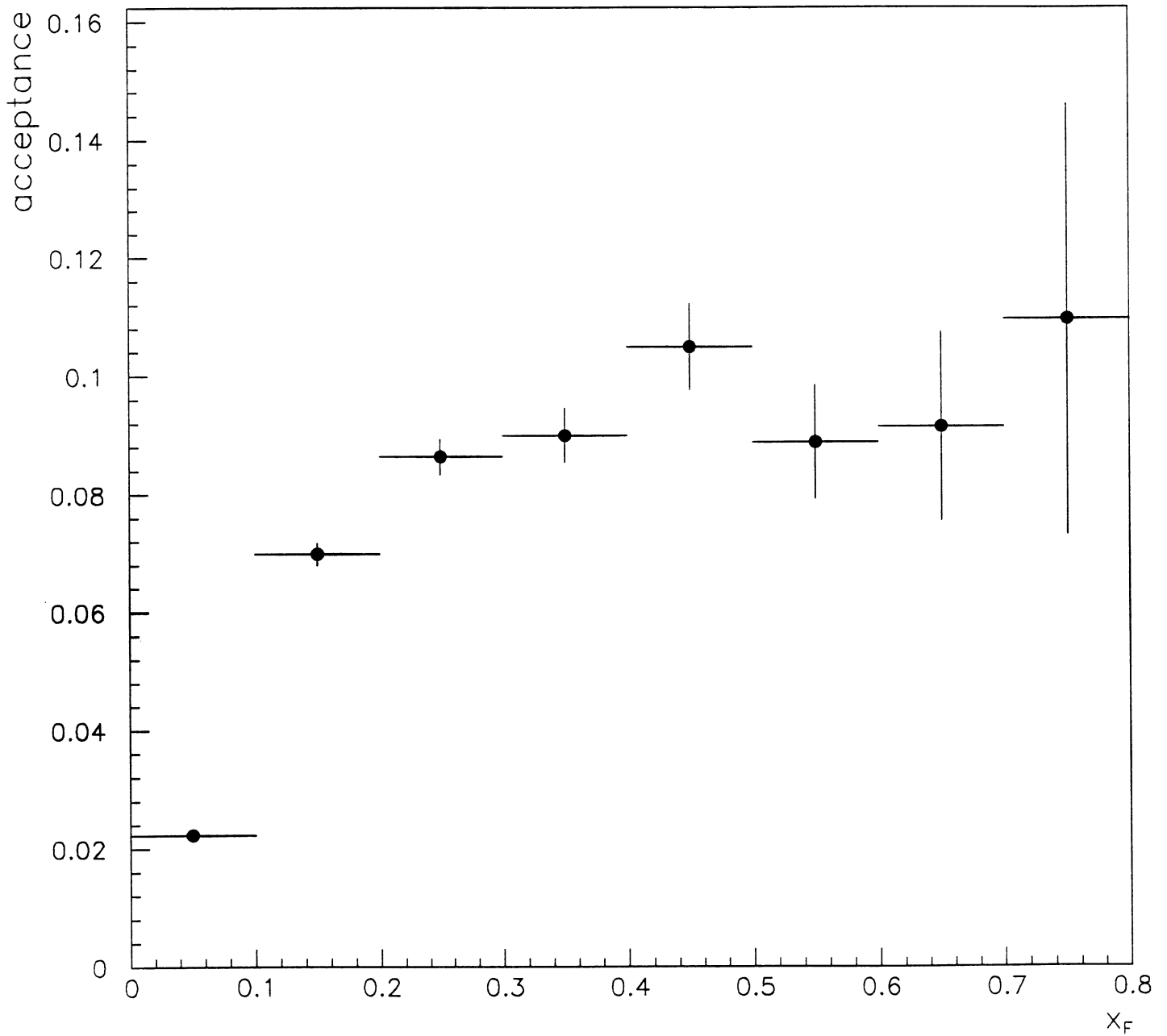
Fig. 2

WA82 - 340 GeV/c π^- beam on W, Cu, Si
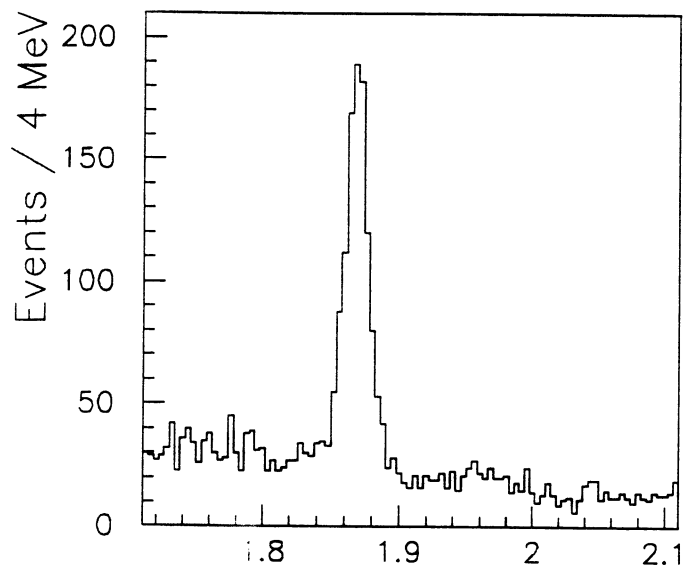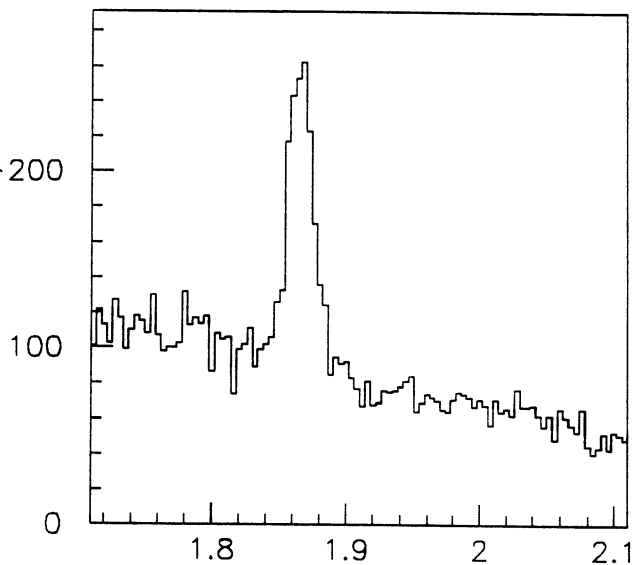
$D^+ \rightarrow K^- \pi^+ \pi^+ + c.c.$

$D^0 \rightarrow K^- \pi^+ + c.c.$
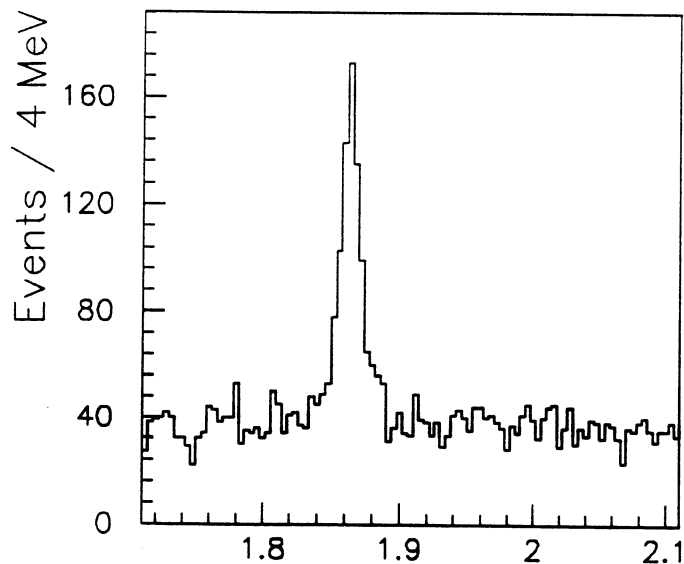
$D^0 \rightarrow K^- \pi^- \pi^+ \pi^- + c.c.$
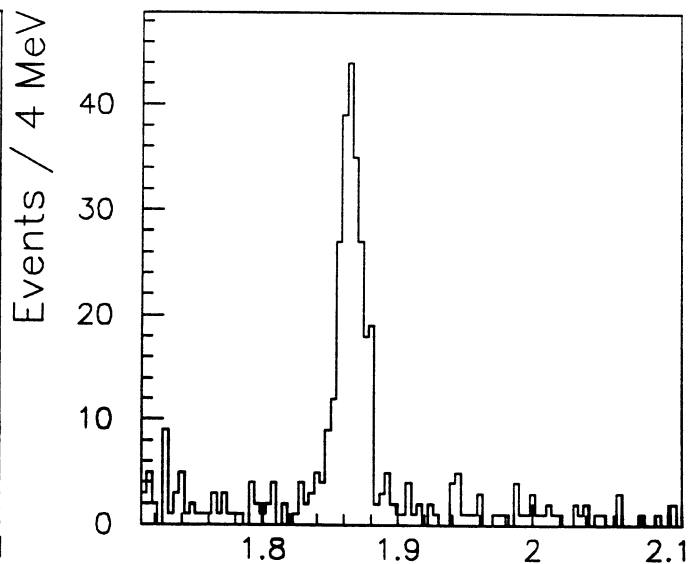
D^0 from $D^{*+} \rightarrow D^0 \pi^+ + c.c.$

$D^+, D_s^+ \rightarrow \phi \pi^+ + c.c.$

$\Lambda_c^+ \rightarrow p K^- \pi^+ + c.c.$

Fig 2
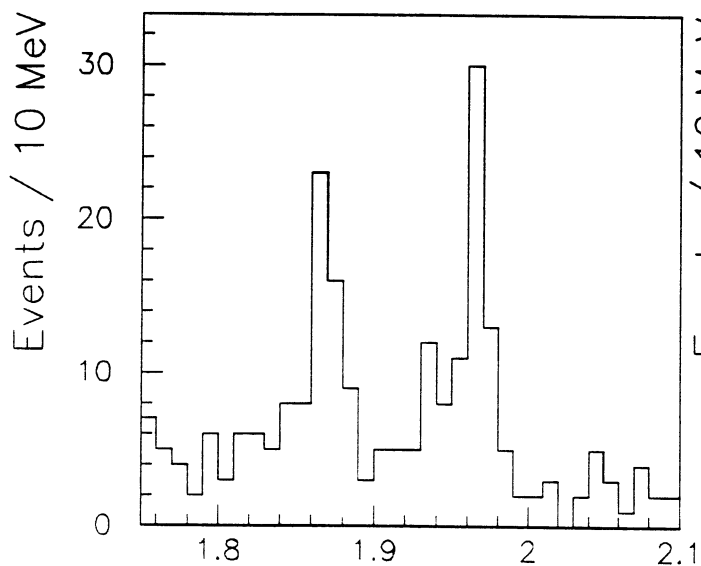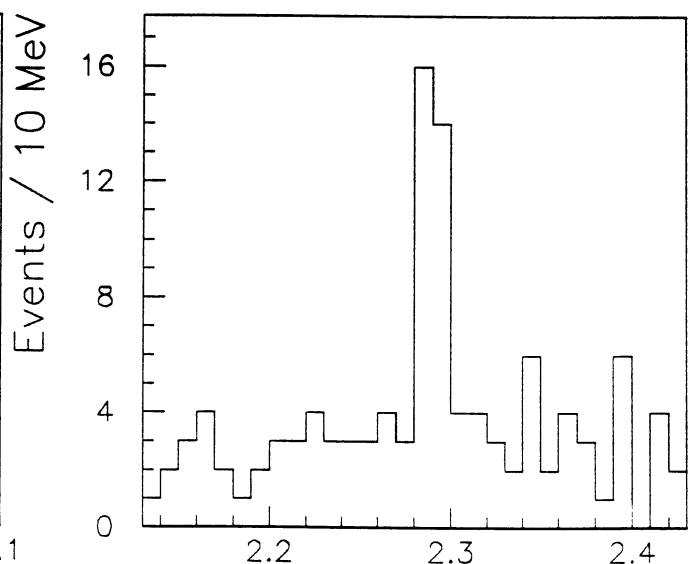
WA82 – 370 GeV/c p beam on W, Si
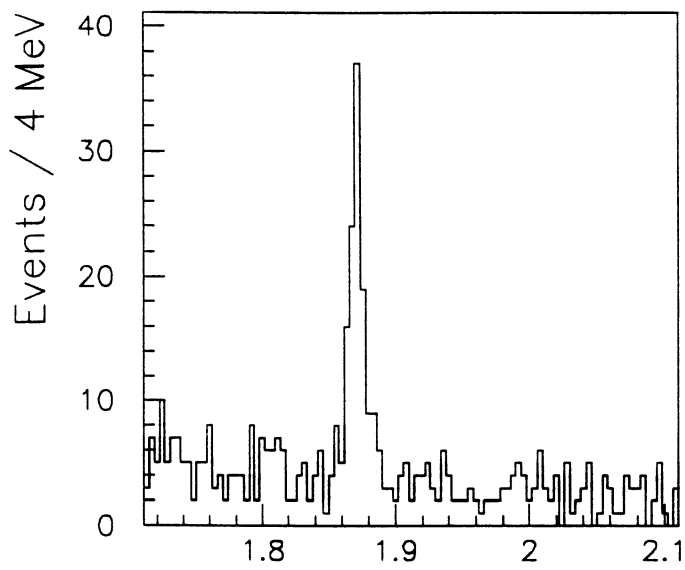
$D^+ \rightarrow K^- \pi^+ \pi^+ + c.c.$
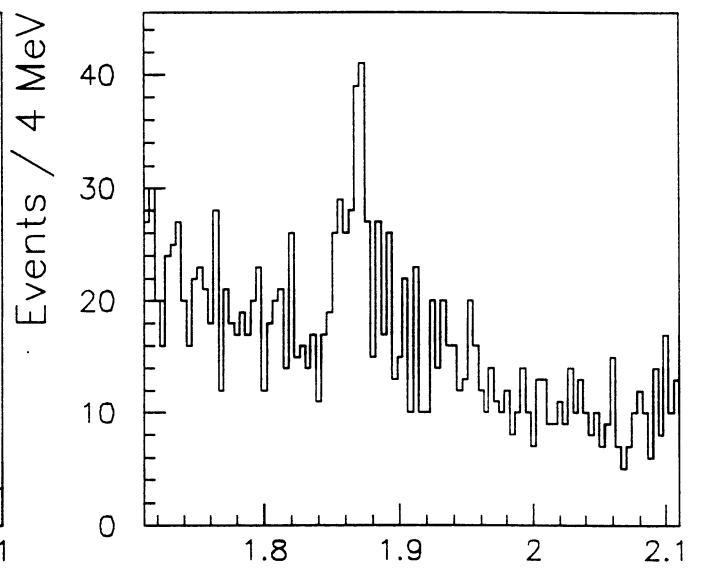
$D^0 \rightarrow K^- \pi^+ + c.c.$
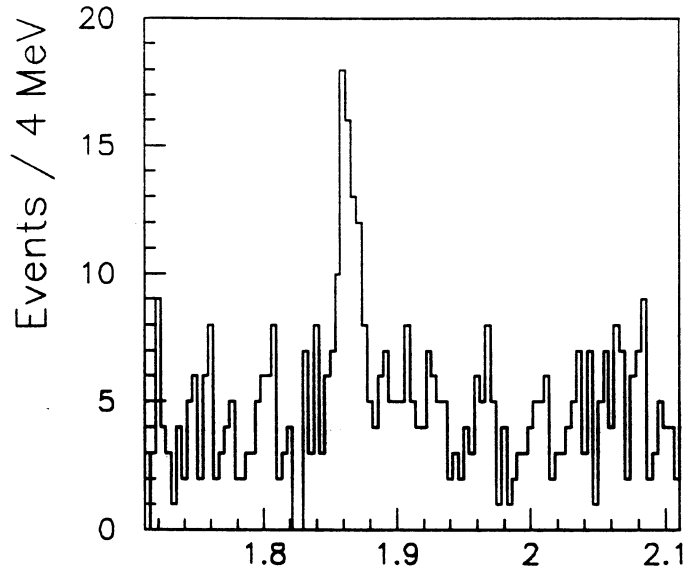
$D^0 \rightarrow K^- \pi^- \pi^+ \pi^- + c.c.$
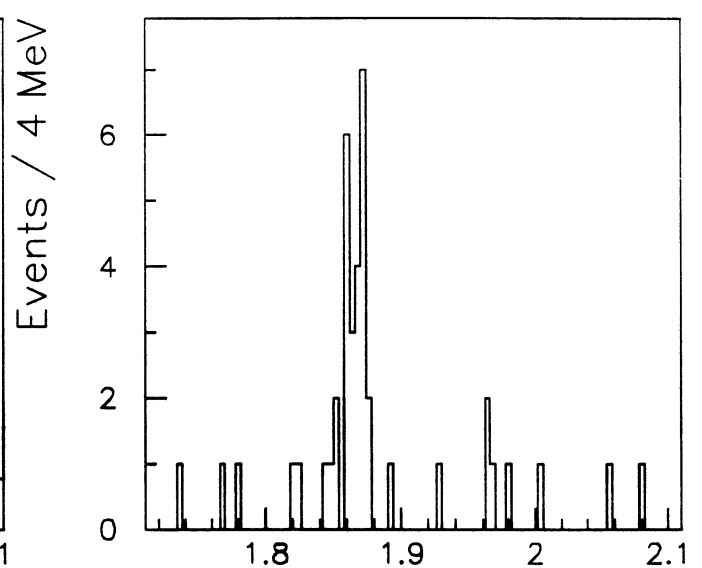
D^0 from $D^{*+} \rightarrow D^0 \pi^+ + c.c.$
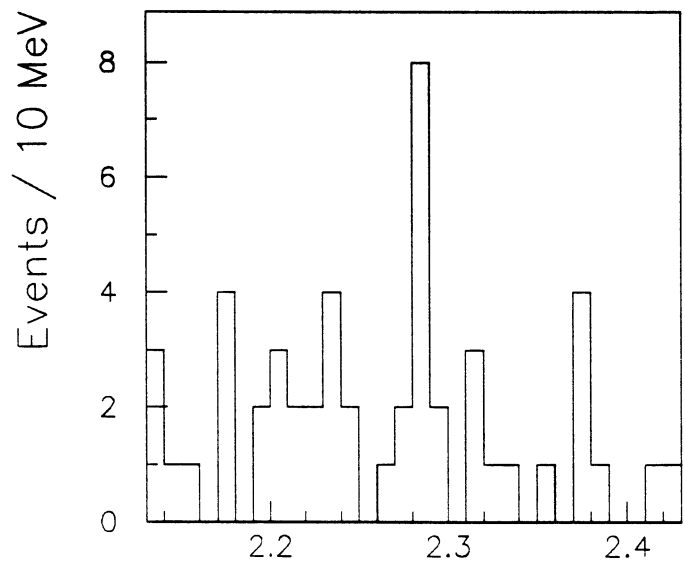
$\Lambda_c^+ \rightarrow p K^- \pi^+ + c.c.$

WA82 − Invariant mass fits − 1987 data
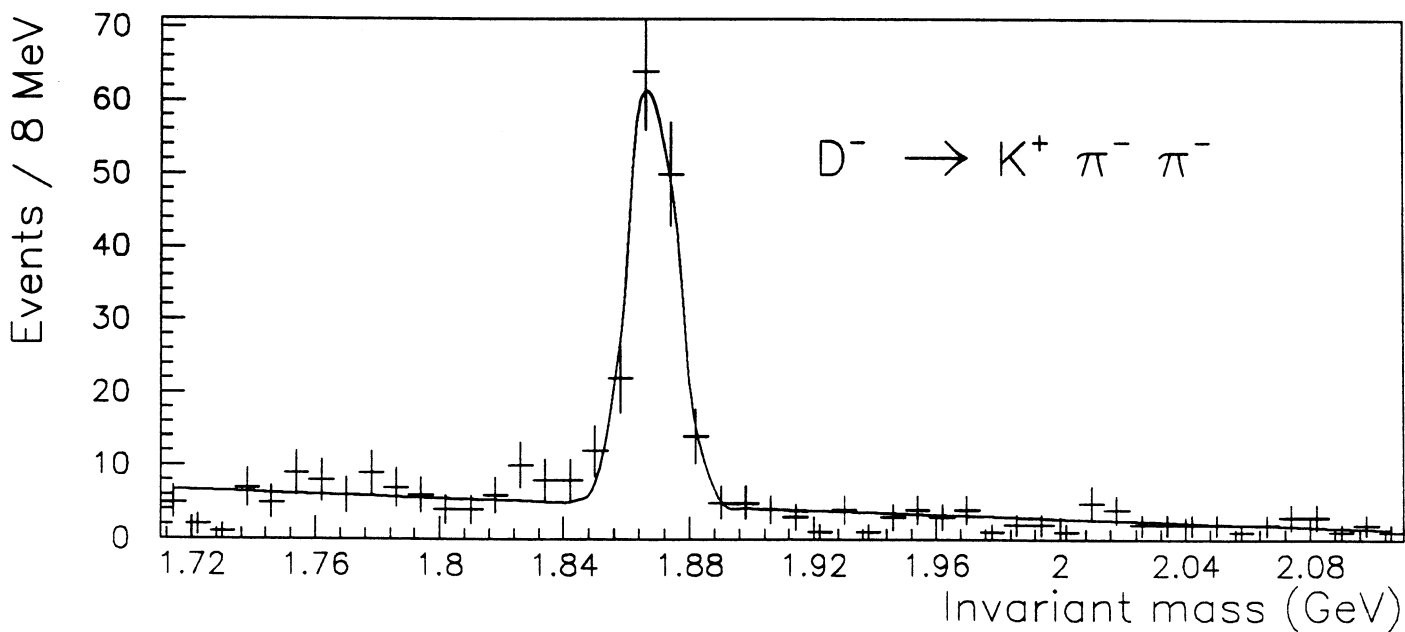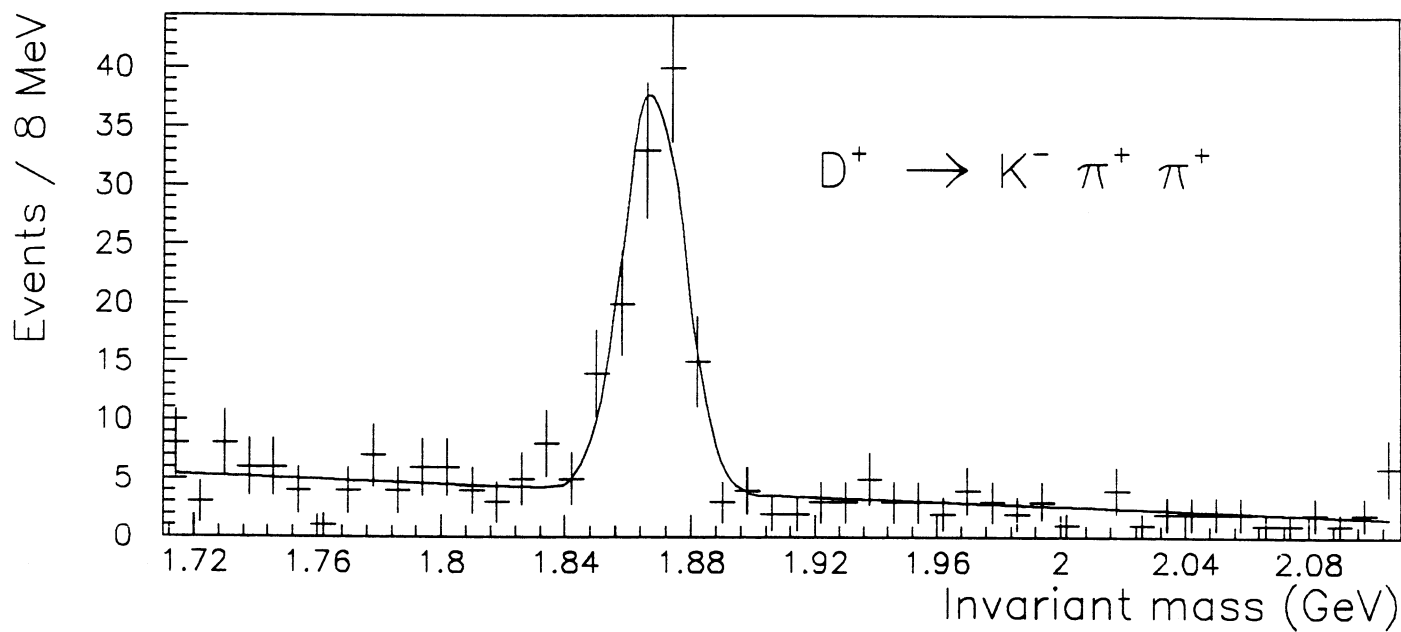
Fig. 5
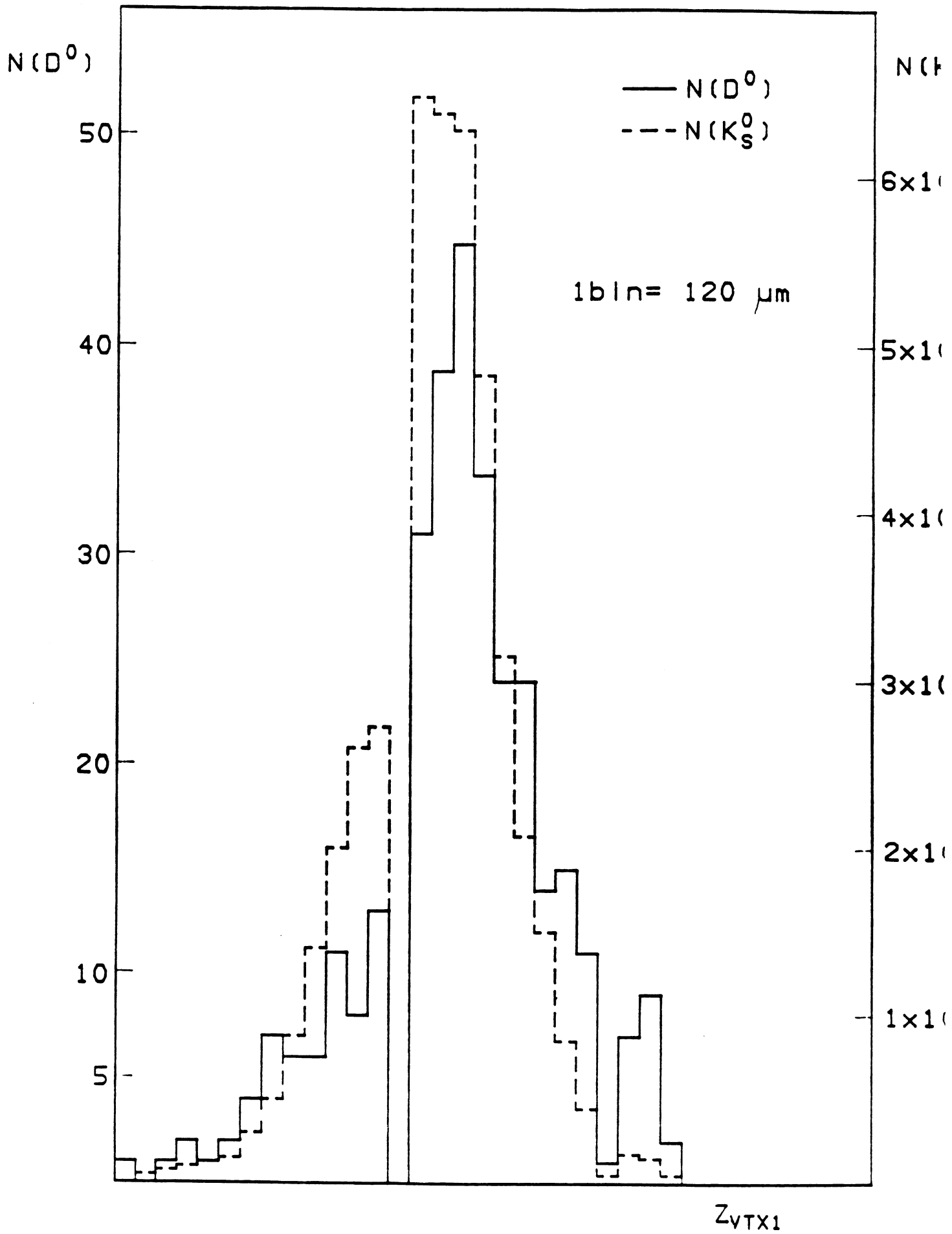
Fig. 6
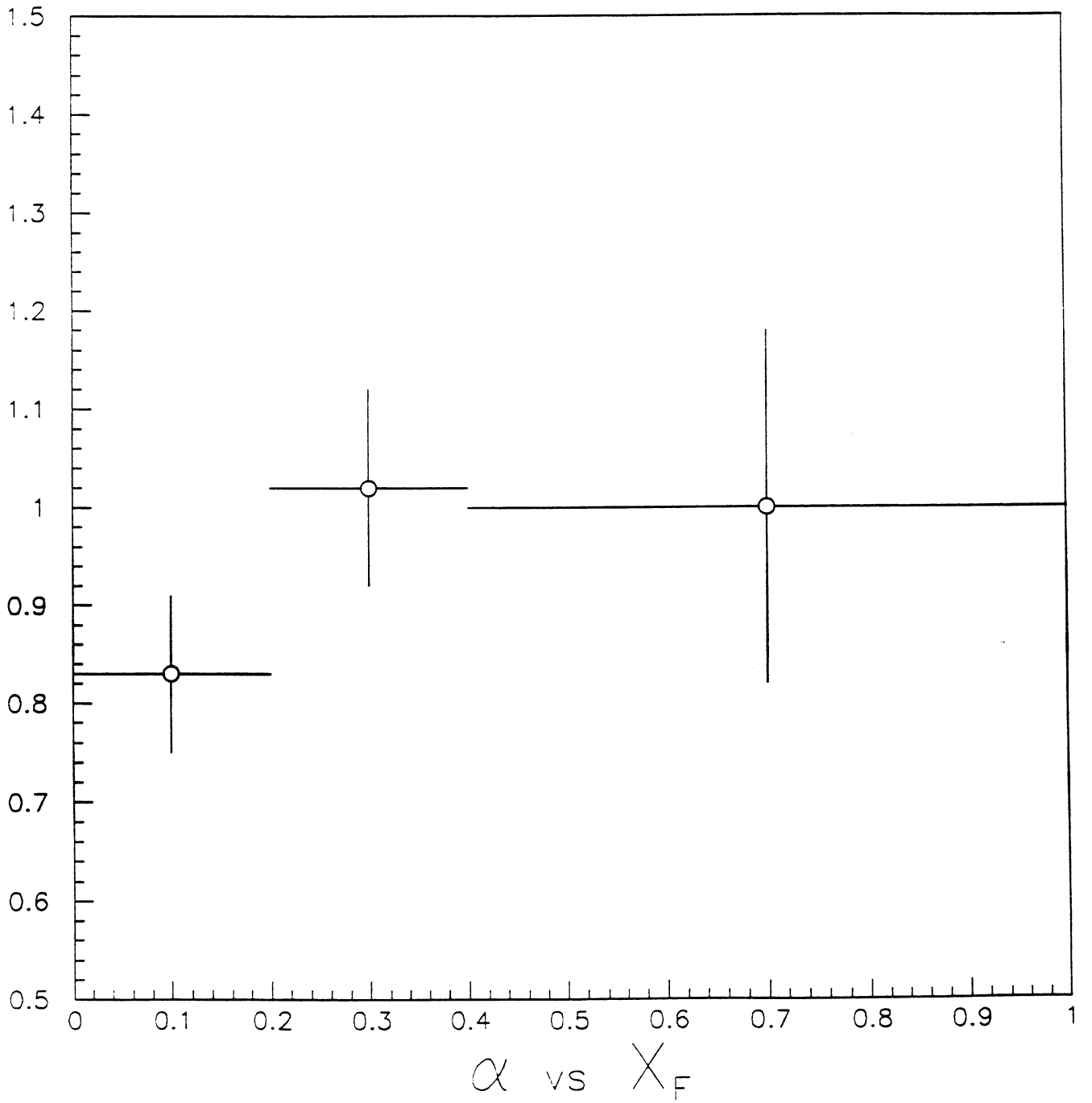
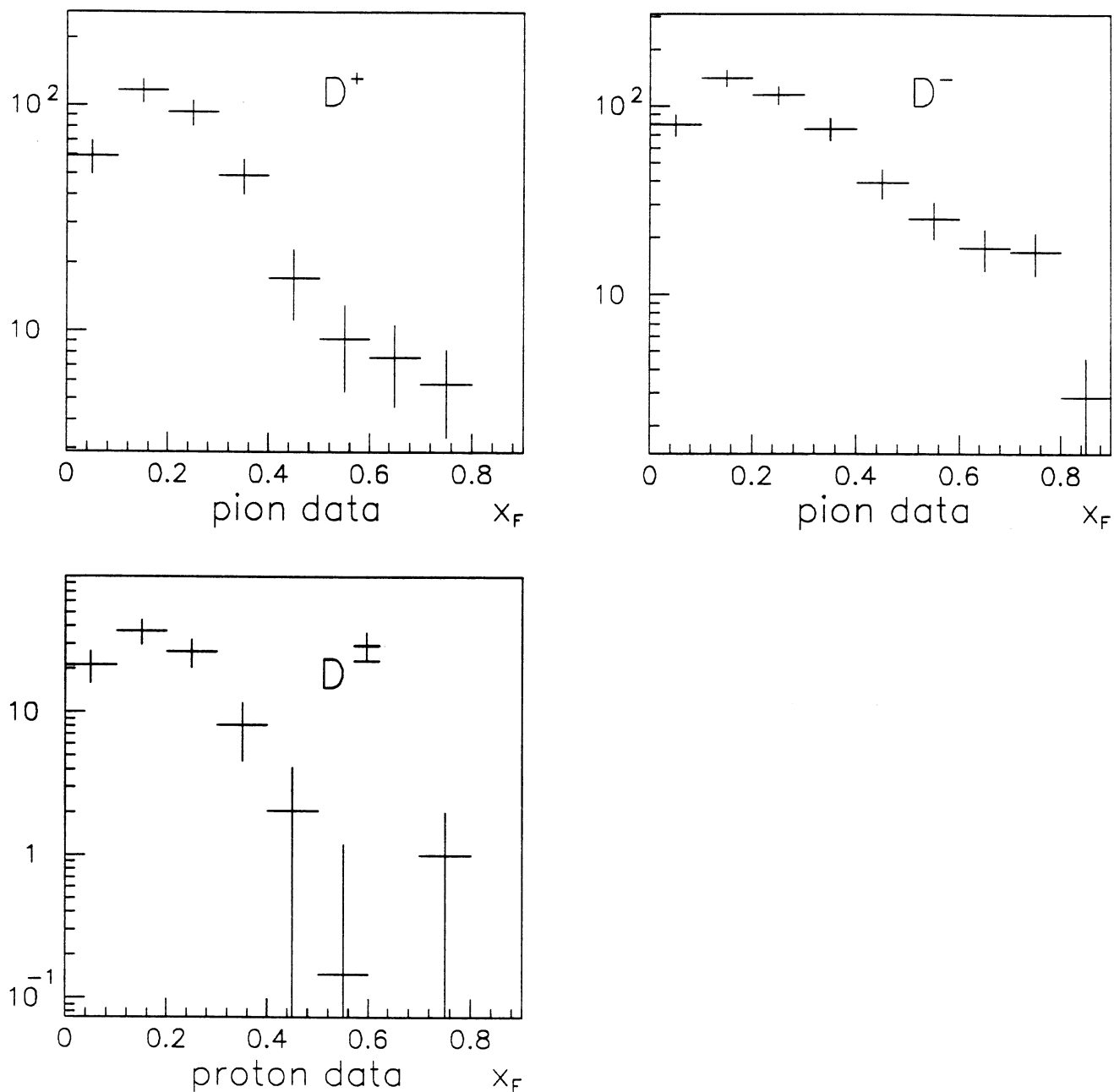Fig. 7

WA82 D$^{\pm}$ x$_F$ distributions (uncorr. for acceptance)
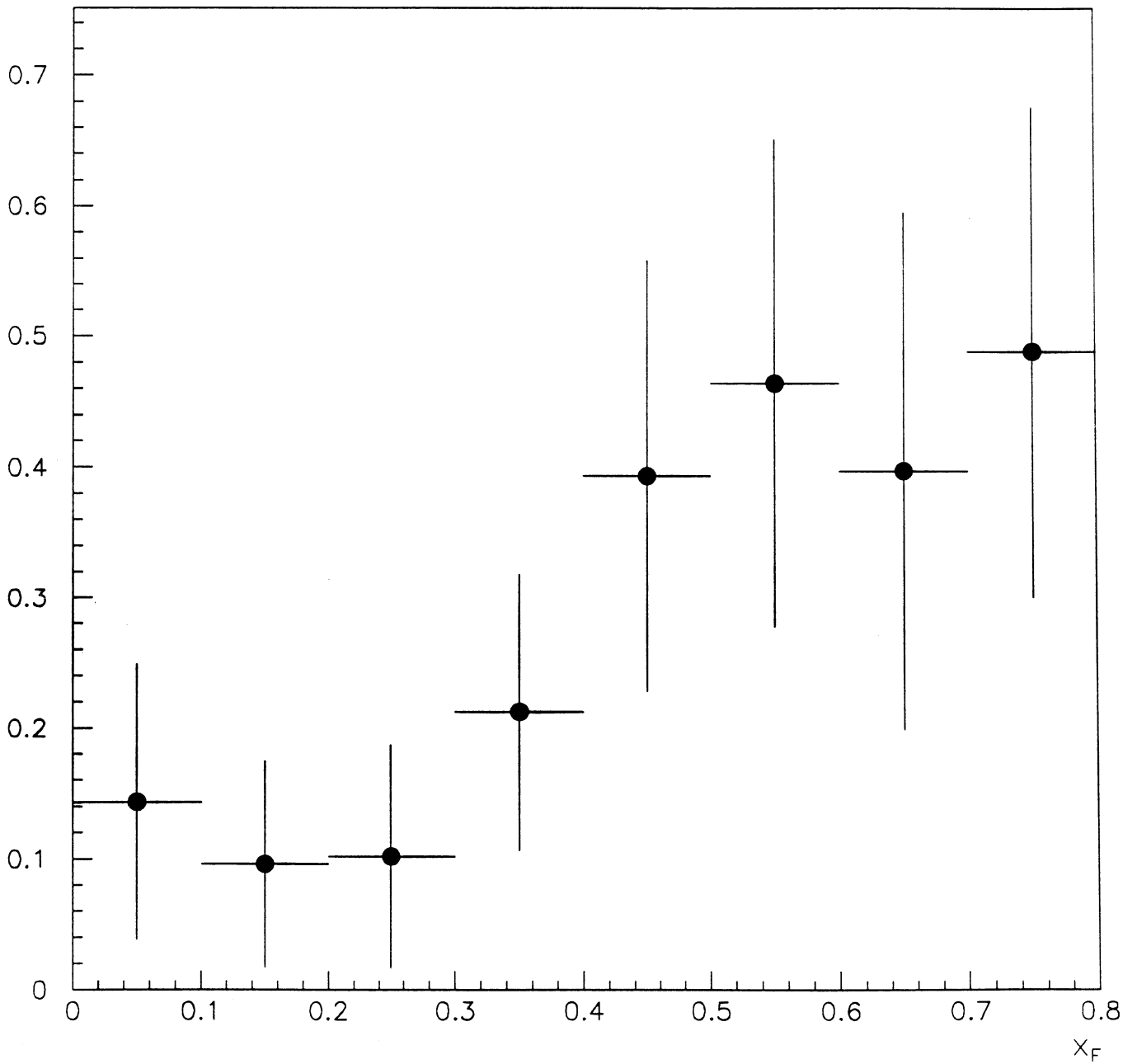

Fig. 8

WA82 $(D^- - D^+) / (D^- + D^+) - \pi^-$ data
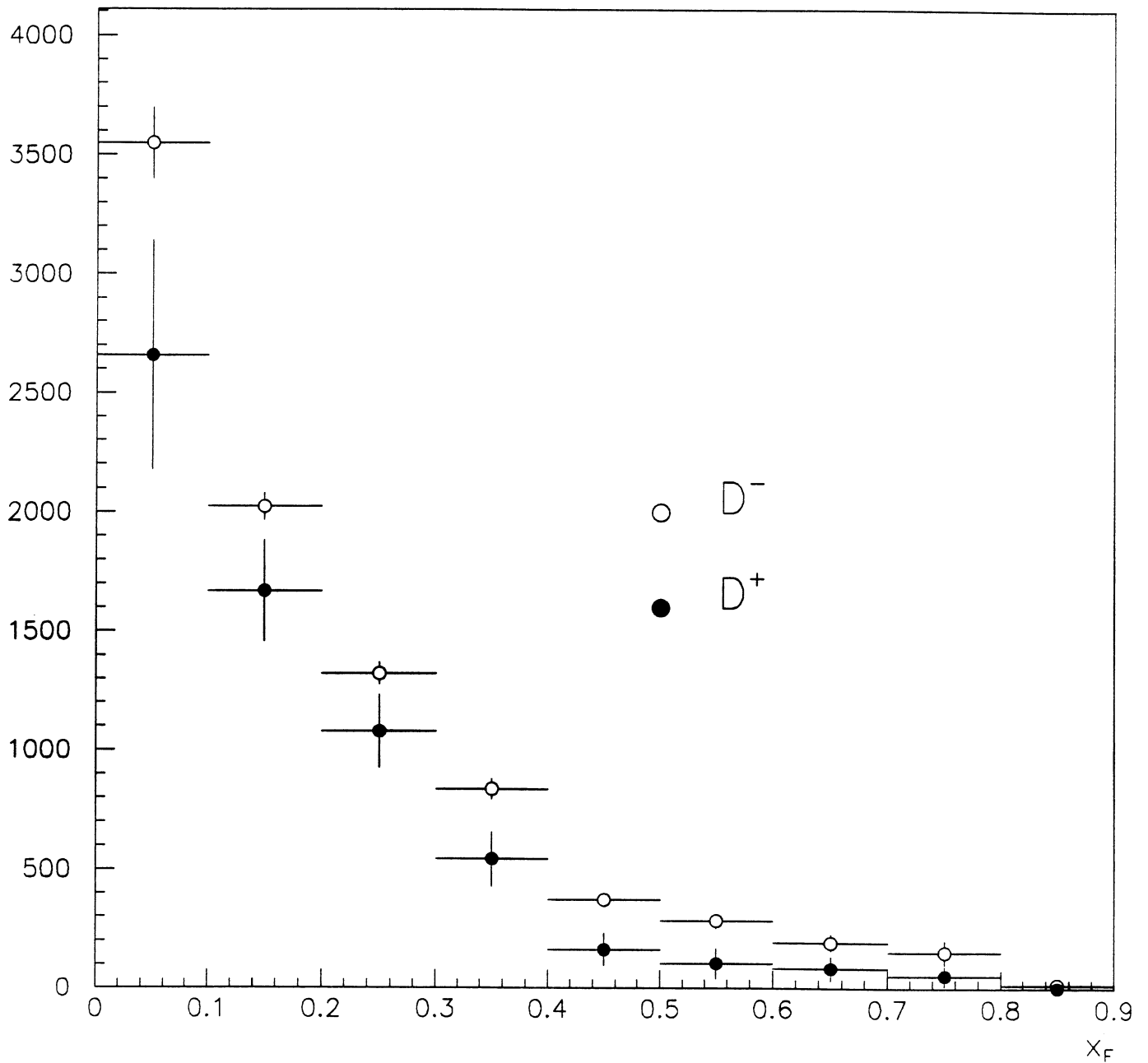
Fig. 8

WA82 $D^{\pm}$ x_F distributions $-$ π^- data
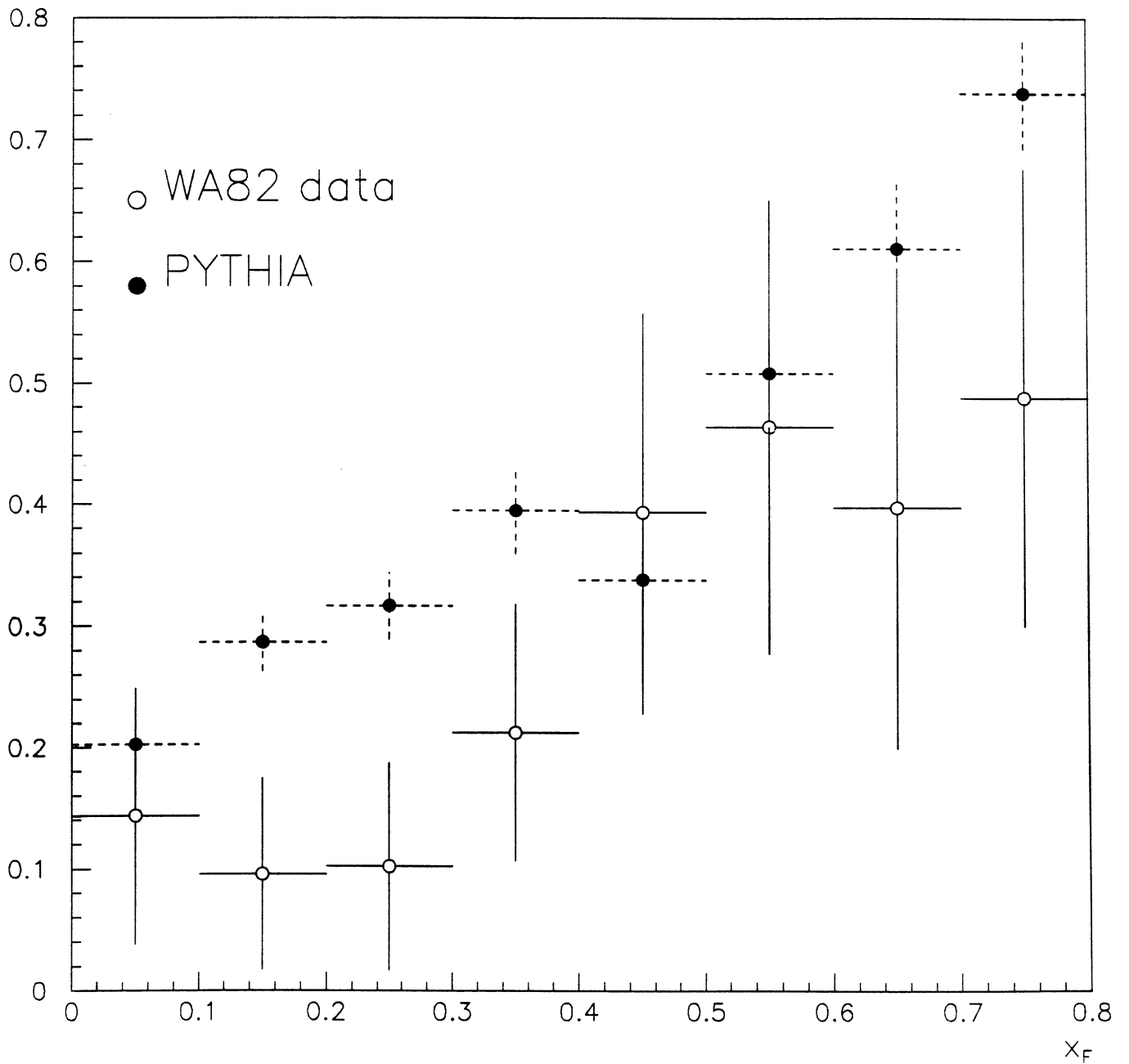
D^-

D^+

x_F

Fig. 10

$$\left(D^- - D^+\right) / \left(D^- + D^+\right) - \pi^- \text{ beam}$$

○ WA82 data

● PYTHIA

X_F

Fig. 11

D^+ x_F distributions $- \pi^- N$ interactions

○ WA82 D^+

● PYTHIA D^+

△ NTLO c

x_F

Fig. 12

D^- x_F distributions $- \pi^-$ N interactions

o WA82 D^-
● PYTHIA D^-
△ NTLO $\bar{c}$

10^2

10

1

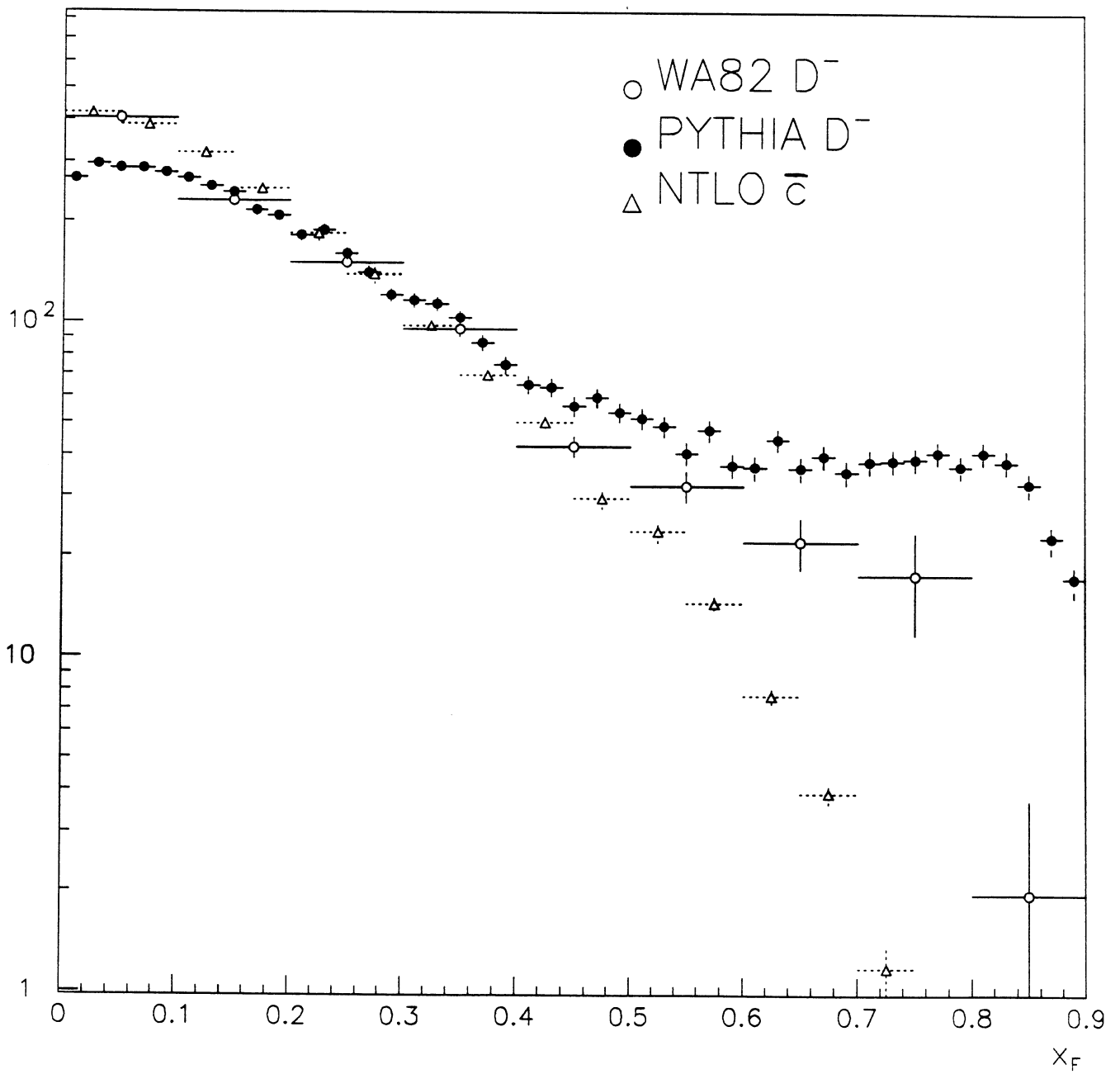0   0.1   0.2   0.3   0.4   0.5   0.6   0.7   0.8   0.9

x_F
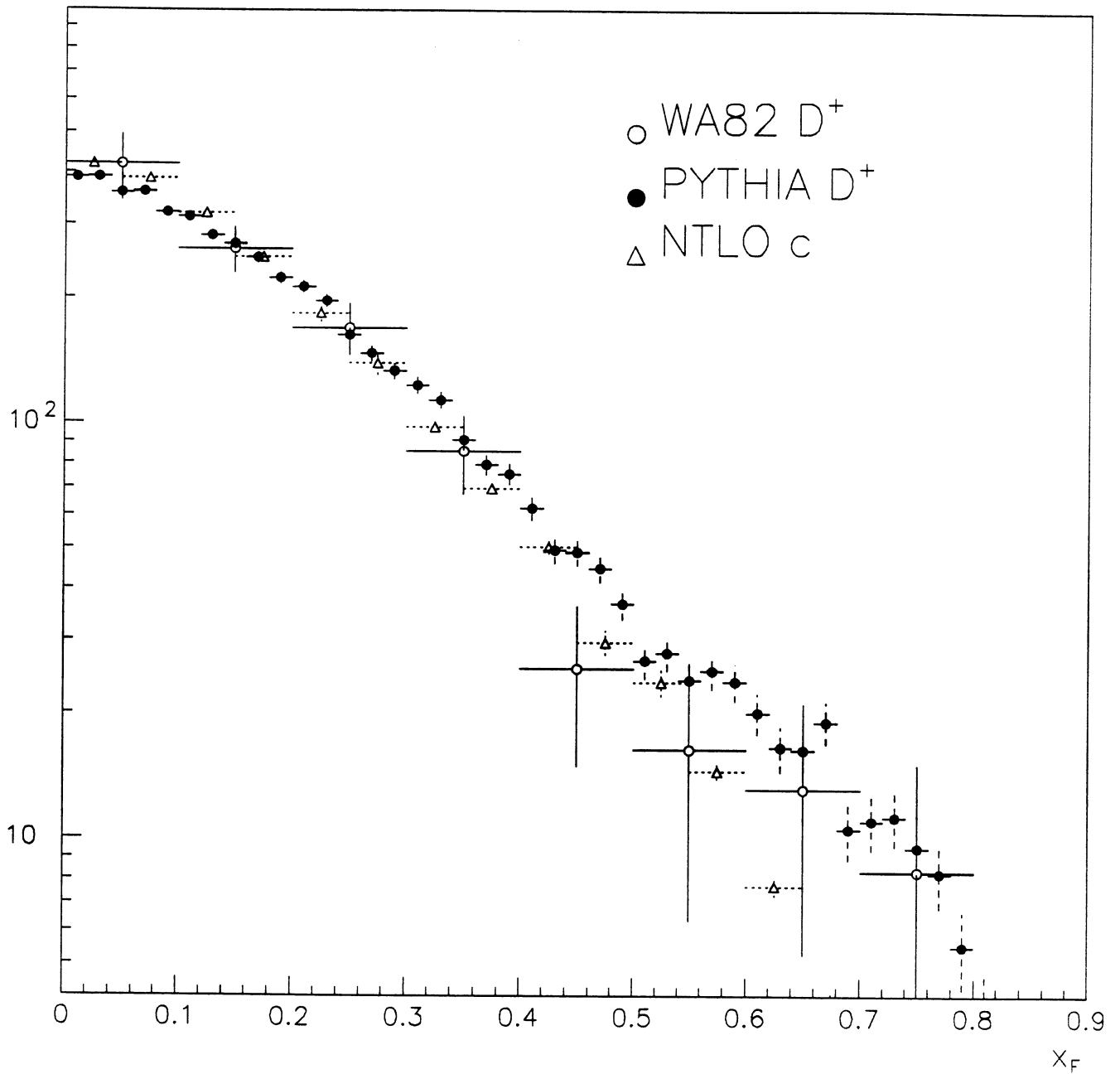
Fig. 13

$D^{\pm}$ x_F distributions — p N interactions

o WA82 $D^{\pm}$
● PYTHIA $D^{\pm}$

x_F

Fig. 14